

The Effect of Surface Composition on the Chemisorption of Hydrogen on Tungsten Carbide

M. BOUDART,¹ J. S. LEE, K. IMURA,² AND S. YOSHIDA³

Department of Chemical Engineering, Stanford University, Stanford, California 94305-5025

Received August 16, 1985; revised June 18, 1986

Polymeric carbon and oxygen were detected at the surface of tungsten carbide powders by Auger electron spectroscopy and electron spin resonance. Chemisorption of dihydrogen is suppressed by polymeric carbon but enhanced by surface oxygen as some of the latter reacts in the presence of water with hydrogen spilling over from the tungsten carbide parts of the surface. © 1987 Academic Press, Inc.

INTRODUCTION

Tungsten carbide, WC, exhibits platinum-like catalytic behavior for some surface and catalytic reactions (1). Although extensive investigations of the last decade have contributed to a better understanding of the bonding and the electronic properties of transition metal carbides (2), the reasons for the platinum-like behavior WC are still unknown. But in a general sort of way, Leclercq *et al.* (3) reasoned that by dissolving a nonmetallic element, e.g., carbon, in a metal of group 6B (tungsten or molybdenum), that chemisorbs molecules too strongly, the surface reactivity of the host metal could be tempered by increasing the electronic density per metal atom of the host. Thus the resulting carbides might catalyze certain reactions because of their ability to bind many organic and inorganic molecules strongly enough but not too strongly. This heuristic idea has been supported by the low pressure study of Ko and Madix, who observed that carbon adlayers on Mo(100) and W(100) single crystal sur-

faces not only suppressed the dissociation of CO and H₂ at room temperature but also modified the rate and selectivity of some surface reactions taking place on the clean metals (4-7).

It is very difficult to prepare tungsten carbide surfaces with ideal stoichiometry. Ross and Stonehart (8, 9) determined the surface composition of WC by Auger electron spectroscopy (AES) and X-ray photoelectron spectroscopy (XPS). In addition to tungsten and carbon, oxygen and other elements were also detected. They studied hydrogen chemisorption and electrocatalytic H₂ oxidation on several WC samples and concluded that the active sites of WC were composed of either carbon-deficient tungsten or of oxygen-substituted carbide. However, Kojima *et al.* reported that their WC was active in the hydrogenation of ethylene only after evacuation above 1270 K which removed the surface oxygen and oxide as revealed by XPS (10). Investigations of Ko and Madix on single crystals of tungsten and molybdenum revealed that carbon, oxygen, and sulfur adatoms reduced the ability of surfaces to chemisorb H₂ and CO (4, 6). The importance of surface composition was underscored by studies (11, 12) that showed that the steady-state rate of ammonia synthesis on various molybdenum powders is reached only after uptake

¹ To whom queries concerning this paper should be sent.

² Present address: JGC Corporation, Yokohama, Japan.

³ Present address: Department of Hydrocarbon Chemistry, Kyoto University, Kyoto, Japan.

of one or two monolayers of surface nitrogen.

Thus, in discussing the surface reactivity and catalytic activity of carbides, the surface cleanliness and composition should be defined. Deviations from stoichiometry involve excess carbon in the form of polymeric ("graphitic") overlayers, oxygen, and excess tungsten (carbon deficiency). The present study deals with hydrogen chemisorption by several WC samples, the surface composition of which was examined by AES and electron spin resonance (ESR).

EXPERIMENTAL

Five kinds of WC powder were obtained from different sources. A commercially available WC was obtained from Sylvania Company (SYL). Other samples were prepared at AEG Telefunken, the National Bureau of Standards (NBS), and Pratt and Whitney Aircraft (PWA). A final one (CMR) was synthesized by a reaction between tungsten hexachloride vapor and butane at a pressure of 1.3 kPa on a tungsten filament at 1613 K. Specific surface areas were measured with dinitrogen by the usual BET method. Crystal structures were obtained by X-ray diffraction.

For ESR spectra at room temperature, a Varian E 3 type spectrometer was used with a 100-kHz field modulation. The magnetic field was calibrated by DPPH powder and also by a standard solution of peroxyamine disulfate.

For AES studies, a Varian AES spectrometer with a four-grid analyzer was used to examine powders that were pressed on a molybdenum screen. A 2-keV, 120-A electron beam was used as the excitation source. The spectrum was recorded at room temperature for a sample which had been previously evacuated at 423 K. Dihydrogen and dioxygen were purified and adsorbed in a system that has been described previously (13). The initial pressure was fixed at 20 kPa. Prior to some of the hydrogen adsorption runs, water was preadsorbed. The water had been degassed as de-

scribed elsewhere (14). The water vapor at a pressure corresponding to its vapor pressure saturated at room temperature was introduced onto a WC sample which had been previously evacuated at 423 K for 1 h. The amount of the water vapor was controlled by changing the gas volume. The water was adsorbed irreversibly at room temperature on the sample up to an amount of at least 50 $\mu\text{mol g}^{-1}$. Indeed, with such amounts of adsorbed water, there was no significant difference on the rate of subsequent hydrogen adsorption with or without prior evacuation for 0.5 at room temperature of the water covered samples. After one measurement of hydrogen adsorption rate, the WC was exposed to 20 kPa dioxygen at room temperature overnight and the above procedure was repeated for another measurement. The above cycle of runs was repeated to ascertain whether changes in amounts or rates of adsorption took place. None could be detected.

RESULTS

Table 1 shows the values of hydrogen uptake and crystal structures. Hydrogen uptake was measured at room temperature by noting the pressure change after a 15 h exposure to dihydrogen. Before these measurements, the samples had been exposed to air at room temperature and then were evacuated at 423 K for 1 h. In order to investigate surface composition, ESR and AES studies were carried out. As shown in Fig. 1, all of the samples gave ESR symmetric singlet signals with g -value between 2.002 and 2.003 and widths between 5 and 7 G. The line shape and parameters indicated that the signals could be assigned to radicals associated with carbonaceous compounds similar to carbon black (15). The radicals seem to be mainly at the surface since the signal intensities decreased by contact with air at room temperature to about two-thirds of those measured under vacuum. In what follows, the carbon associated with this signal will be called polymeric carbon to differentiate it from the

TABLE 1
Characteristics of Tungsten Carbide Samples

WC	Surface area ($\text{m}^2 \text{g}^{-1}$)	Hydrogen uptake ^a ($\mu\text{mol m}^{-2}$)	Crystal structure	
			Crystal system	Lattice constant
				a_0 (pm)
AEG	6.3	5.0	Hexagonal	290.1 288.4
NBS	0.8	4.5	Hexagonal	290.5 283.6
SYL	3.3	1.3	—	— —
PWA	5.5	0.4	Hexagonal	290.1 283.0
CMR	15	0.1	Cubic	— —

^a The sample was preexposed to dioxygen and then evacuated at 423 K for 1 h.

carbide carbon associated with the carbide structure. We believe that the adjective polymeric is preferable to the other commonly used one: graphitic. Quantitative analysis was not attempted in this study. However, it is obvious that the CMR sample contains a large amount of polymeric carbon.

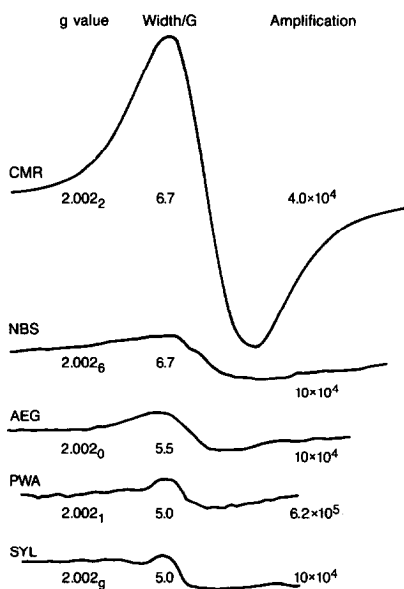


FIG. 1. ESR spectra of tungsten carbide samples *in vacuo*.

The AES signals of the WC samples are shown in Fig. 2. As also reported by Ross and Stonehart, not only tungsten and carbon peaks but also sulfur and oxygen peaks were observed. The most interesting feature of the spectra is the line shape of the carbon *KLL* transitions in the vicinity of 270 eV. We can clearly divide the samples into two groups by the lineshape. Samples from AEG, NBS, and SYL gave a triplet signal, while PWA and CMR gave a singlet signal. Many AES studies of metal carbides agree that carbide carbon gives a charac-

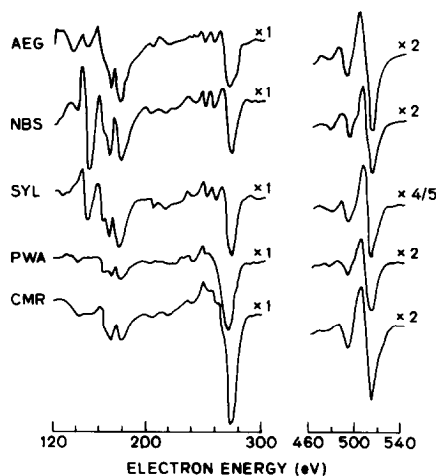


FIG. 2. AES signals of tungsten carbide samples.

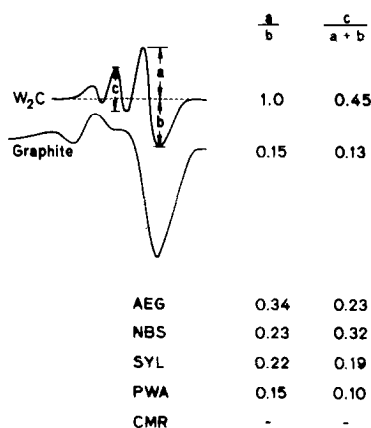


FIG. 3. Shape parameters of carbon *KLL* transition.

teristic triplet signal similar to that of the former materials (AEG, NBS, SYL), while it is well known that polymeric or graphitic carbon gives a singlet signal like that of the latter materials (PWA, CMR) (16).

A relative contribution of polymeric and carbidic carbons to carbon *KLL* transition can be estimated by examining the detailed variation of peak shape (17, 18). Figure 3 defines shape parameters with the ratios of a/b and $c/(a+b)$ and lists corresponding values for WC samples. The spectra and shape parameters for standard graphite and W₂C are also shown. Despite a characteristic triplet signal for active samples (AEG, NBS, and SYL), the values of shape parameters are much less than those of W₂C standard, indicating that a mixture of polymeric and carbidic carbon exists. On the other hand, the peak shape of PWA and CMR samples and the value of shape parameter for PWA sample are very close to those of graphite standard. Also N₅/N₆/N_{6,7} transition of W (9) at 163 eV are much more diffuse than for active samples. These indicate that multilayers of polymeric carbon are covering most of the surface. A very clear qualitative correlation exists between the hydrogen uptake and the proximity of shape parameters to those of W₂C standard. A similar correlation is also seen between the hydrogen uptake and intensity of W Auger peaks.

With respect to oxygen as revealed by AES, a triplet signal due to oxygen was found for all samples and the signal was very stable. Dihydrogen treatment at room temperature and a pressure of 20 kPa, followed by an evacuation at 423 K, caused little change in the oxygen peak of AEG. In addition, dihydrogen treatment at 573 K hardly affected hydrogen uptake. These results suggest that the majority of the oxygen existed as an oxide layer on the surface. It has been observed previously that X-ray amorphous surface oxide could be formed on WC by contact with atmospheric dioxygen (19). It is therefore interesting to examine the role of surface oxygen for the reactivity of WC. Again, hydrogen chemisorption was carried out at room temperature using AEG and SYL. This time various amounts of water were introduced into the system as described in the previous section. As shown in Fig. 4, it is obvious that the adsorption rates depended greatly on the amount of preadsorbed water. With an increase in the amount of preadsorbed water, the rate went up remarkably. However, the amounts of hydrogen uptake at equilibrium were constant. The value for AEG samples was about 100 $\mu\text{mol g}^{-1}$, which

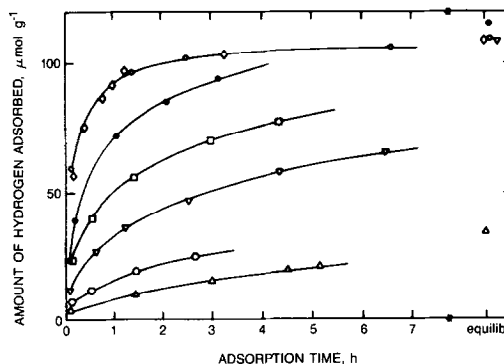


FIG. 4. The effect of water on hydrogen adsorption by AEG-WC: (1) exposed to H₂O (2.67 kPa) after evacuation; (2) evacuated at 423 K, exposed to O₂, but not to H₂O and evacuated at room temperature. Evacuation temperature (K) and H₂O adsorbed ($\mu\text{mol g}^{-1}$): (○) 296, >50; (△) 423, 0; (◐) 423, 5; (▽) 423, 10; (◑) 423, 25; (◇) 423, >50; (●) —, 50.

means 2.0×10^{15} atom cm^{-2} . This is approximately twice the value for platinum. Hydrogen chemisorption on SYL gave the same result, i.e., the rate increased after preadsorption of water and the equilibrium amount of hydrogen uptake was constant, although the value was lower than that of AEG. It has been reported that water could accelerate the reduction of tungsten trioxide WO_3 to tungsten bronze at room temperature in the presence of platinum mixed with WO_3 , and it has been concluded that hydrogen spillover took place from platinum metal to WO_3 (14, 20). Our present result can be explained in the same way. Thus, tungsten oxide may have existed in the surface region and reacted with hydrogen spilling over WC at room temperature, at rates increased by water vapor.

The data on oxygen adsorption are shown in Fig. 5. Before the measurements, hydrogen was preadsorbed at room temperature to equilibrium with adequate amounts of water. The amount of oxygen uptake by the AEG sample after the evacuation at room temperature was $50 \mu\text{mol g}^{-1}$. Clearly, the preadsorbed water had less effect on the rate of adsorption of oxygen than on that of hydrogen. From the difference of equilibrium uptake, it seems that one-third of the preadsorbed hydrogen was desorbed by evacuation at 423 K.

DISCUSSION

It is clear that both PWA and CMR samples are covered with polymeric carbon. There was no significant difference in line shape between the carbon KLL transition signals of PWA and CMR samples in Fig. 2, showing that the bonding character of carbon in both samples is similar. From the ESR measurements, the spin density in the CMR sample could be estimated to be ten times larger than that in the PWA sample. The origin of spins in carbon black is believed to be unpaired electrons stabilized in condensed aromatic rings (21). This compound could be the source of the carbon signal in the AES spectra of CMR. It is well

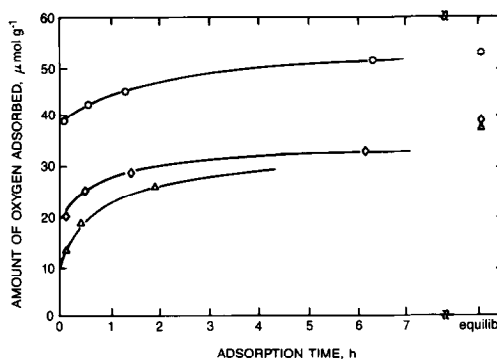


Fig. 5. The effect of water on oxygen adsorption by AEG-WC. (○) Exposed to H_2 , then evacuated at room temperature; (Δ) exposed to H_2 , then evacuated at 423 K; (\diamond) exposed to H_2 , then evacuated at 423 K, and exposed to H_2O (2.67 kPa), then evacuated at room temperature.

known that a graphitization of the condensed aromatic rings of charred carbon black causes a decrease in ESR signal. The PWA sample could be covered with partially graphitized polymeric carbon. Since the bonding character of carbon in the condensed aromatic ring and graphite is the same, it is natural that both samples were almost identical in the line shape of their AES signals.

A clear qualitative correlation exists between the hydrogen uptake and the carbon species. The tungsten carbide with polymeric carbon on the surface was essentially inactive in hydrogen adsorption at room temperature. The primary factor controlling the apparent reactivity with respect to dihydrogen is therefore surface contamination by polymeric carbon.

The hydrogen uptake of SYL was about one-third of that for AEG and NBS. In Fig. 2, the oxygen peak of SYL is seen to be much larger than that of AEG and NBS. An explanation for this may be that SYL was provided after it had been milled for 24 h to get a fine powder. The process is likely to cause surface oxidation. The suspected oxide layer, in addition to polymeric carbon, may have decreased the hydrogen uptake shown in Table 1.

As mentioned in the previous section, preadsorbed water increases the rate of hydrogen adsorption by accelerating hydrogen spillover from WC sites to the neighboring tungsten oxide, forming a tungsten bronze H_xWO₃. After the hydrogen adsorption reached equilibrium in the presence of water, the AEG sample was evacuated at 423 K to remove most of the water. The sample, however, would still have contained the hydrogen in the tungsten bronze as well as the residual hydrogen which was not desorbed during the evacuation. The AEG sample was then exposed to dioxygen (but not to water), and finally evacuated at room temperature. Hydrogen adsorption was then measured again (black circles in Fig. 4). Although the AEG sample was not exposed to water, a large increase in the rate and equilibrium amount of hydrogen adsorption was observed relative to the initial hydrogen adsorption without water. Therefore, water must have been produced when the sample was exposed to dioxygen before hydrogen adsorption. It appears that adsorbed hydrogen on WC and the hydrogen in the tungsten bronze reacted with dioxygen. Comparison between the amounts of oxygen uptake and of preadsorbed hydrogen shows that the reaction between these species proceeds stoichiometrically. These results show that all the hydrogen which was adsorbed could contribute to make water by reacting with dioxygen.

It is clear from Fig. 4 that the hydrogen in the tungsten bronze might account for a large fraction of the total hydrogen uptake by the AEG sample in the presence of water. Approximately 70% of the total hydrogen could be due to spilled-over hydrogen. If the composition of tungsten bronze was H_{0.35}WO₃ (20), rough calculation indicates that nearly 10% of the tungsten was oxidized. Chemical analysis of the AEG sample agrees with the above estimate. In the case of the SYL sample, although the AES surface oxygen concentration was higher than that of the AEG sample, chemical

analysis showed that the total oxygen content of SYL was about half that of AEG. Therefore, only very thin surface layers of SYL were oxidized, which could result in less hydrogen uptake than by AEG, since the contribution of spillover hydrogen should be less on a heavily surface-oxidized sample.

As mentioned, a considerable part of preadsorbed hydrogen may have existed as tungsten bronze, which itself is stable in air at room temperature. However, in the presence of WC, the hydrogen in tungsten bronze easily reacted with dioxygen at room temperature. Thus, reversed hydrogen spillover from tungsten to WC seems to occur during oxygen adsorption. The preadsorbed water had less effect on the oxygen adsorption rate than that on the hydrogen adsorption. This could be explained as follows. During oxygen adsorption, hydrogen from the tungsten bronze located close to WC reacted with dioxygen to produce water which accelerated the reversed spillover. On the other hand, during hydrogen adsorption, the amount of preadsorbed oxygen was probably very small. Thus, water was not produced in enough quantities to accelerate the hydrogen spillover from WC to tungsten oxide. Therefore, the difference in the oxygen adsorption rates with and without water was small as compared to that observed for hydrogen adsorption.

CONCLUSIONS

The reactivity at room temperature of WC surfaces toward dihydrogen is decreased by polymeric carbon evidenced by AES and ESR. Surface oxygen, bound to tungsten, reacts with hydrogen spilling over from WC sites capable of dissociating dihydrogen. This explains previous observations on hydrogen adsorbed on WC (1). Hydrogen spillover is accelerated by water vapor, as in the well-understood case of Pt/WO₃ mixtures. This study reinforces earlier conclusions that the surface reactivity of tungsten carbide powders is dominated by the nonstoichiometry of their surfaces. Ex-

cess of carbon blocks reactive WC sites. Excess of tungsten reacts with oxygen irreversibly. Although the surface tungsten oxide can be reduced at room temperature with dihydrogen, the latter seems to be provided by water accelerated spillover from WC sites needed to split dihydrogen.

ACKNOWLEDGMENTS

This work was initiated with support from the Center for Materials Research at Stanford University under the NSF-MRL Program. It has been completed with the help of DOE Grant DE-AT03-79ER10502-03. The samples of WC denoted as CMR-WC were made at Stanford by Dr. T. Barbee.

REFERENCES

1. Levy, R., and Boudart, M., *Science* **181**, 547 (1973).
2. Oyama, S. T., and Haller, G. L., *Surface and Defect Properties of Solids*, Specialist Periodical Reports, The Chemical Society, London, **5**, 333, (1982).
3. Leclercq, L., Imura, K., Yoshida, S., Barbee, T., and Boudart, M., in "Preparation of Catalysts, II" (B. Delmon, P. Grange, P. A. Jacobs, and G. Poncelet, Eds.), p. 627. Elsevier, Amsterdam, 1978.
4. Ko, E. I., and Madix, R. J., *Surf. Sci.* **109**, 221 (1981).
5. Ko, E. I., and Madix, R. J., *J. Catal.* **73**, 161 (1982).
6. Ko, E. I., and Madix, R. J., *J. Phys. Chem.* **85**, 4919 (1981).
7. Ko, E. I., and Madix, R. J., *Surf. Sci.* **112**, 373 (1981).
8. Ross, P. N., and Stonehart, P., *J. Catal.* **39**, 298 (1975).
9. Ross, P. N., and Stonehart, P., *J. Catal.* **48**, 42 (1977).
10. Kojima, I., Miyazaki, E., Inoue, Y., and Yasumori, I., *J. Catal.* **59**, 472 (1979).
11. Oyama, S. T., and Boudart, M., *J. Res. Inst. Catal., Hokkaido Univ.* **28**, 305 (1980).
12. Boudart, M., Oyama, S. T., and Leclercq, L., in "Proceedings, 7th International Congress on Catalysis, Tokyo, 1980" (T. Seiyama and K. Tanabe, Eds.), Vol. 1. Elsevier, Amsterdam, p. 578, 1980.
13. Benson, J. E., and Boudart, M., *J. Catal.* **4**, 704 (1965).
14. Levy, R. B., and Boudart, M., *J. Catal.* **32**, 304 (1974).
15. Agler, R. S., "Electron Paramagnetic Resonance Technique and Application." Chap. 7. Interscience, New York, 1968.
16. Haas, T. W., Grant, J. T., and Dooley, G. J., III, *J. Appl. Phys.* **43**, 1853 (1972).
17. Ishikawa, K., and Tomida, Y., *J. Vac. Sci. Technol.* **15**, 1123 (1978).
18. Bliznakov, G. M., Kiskinova, M. P., and Surnev, L. N., *J. Catal.* **81**, 1 (1983).
19. Svata, M., and Zabransky, Z., *Powder Technol.* **11**, 183 (1975).
20. Benson, J. E., and Kohn, H. W., and Boudart, M., *J. Catal.* **5**, 307 (1966).
21. Collins, R. L., Bell, M. D., and Kraus, G., *J. Appl. Phys.* **30**, 56 (1959).